3GPP New Radio Precoding in NGSO Satellites: Channel Prediction and Dynamic Resource Allocation

Thang X. Vu*, Sovit Bhandari*, Mario Minardi*, Hieu Van Nguyen†, and Symeon Chatzinotas*
* The Interdisciplinary Centre for Security, Reliability and Trust (SnT), University of Luxembourg, L-1855 Luxembourg. E-mail: {thang.vu, sovit.bhanhari, mario.minardi, symeon.chatzinotas}@uni.lu
† Danang University of Science and Technology, Da Nang, Vietnam. Email: nvhieu@dut.udn.vn

***Abstract*—The advanced payload technology has opened up a new way to design future NGSO satellite systems exploiting the full flexibility in radio resource and beam coverage management. Conventional spatial multiplexing techniques, which require the CSI, however, cannot be efficiently applied in NGSO due to long round-trip time(RTT). In this paper, we tackle the long RTT in the precoding design by proposing a joint channel prediction and dynamic radio resource management framework. Our aim is to optimize the bandwidth and transmit power in every spot beam based on the predicted channel gains to maximize the system capacity. Since the satellite's orbit is time-varying but predictable, Kalman filter-based channel estimation method is employed. Given the predicted channels, a joint bandwidth allocation and precoding design is formulated. The effectiveness of the proposed framework is demonstrated via practical satellite channel models using the STK software and 3GPP codebook- and non-codebook-based precoding designs.**

***Index Terms*—NGSO satellites, LEO, MEO, flexible payload, channel estimation, 3GPP, resource allocation.**

I. Introduction

Satellite services combined with 5G mobile telecommunications can take advantage of extended service coverage to provide 5G services in cost-effective ways in areas where terrestrial network services are vulnerable. They also provide service continuity for passengers on mobile platforms (aircraft, ships, high-speed trains, buses, etc.), which results in the support of reliable 5G service anywhere. The 3GPP Release 17 [1] has endorsed the integration of satellites (and other Non-Terrestrial Networks (NTN)) as a part of the 5G ecosystem involving both cellular and satellite stakeholders. Multiuser precoding is one of the key multiuser techniques in 5G and beyond networks towards high data rate, ubiquitous coverage and high energy efficiency. The latest release of the 5G New Radio (NR) standard offers a very dynamic and flexible framework in terms of framing structure, frequency duplexing, and control signaling to support multi antenna and beam management techniques [2]. For now, the NR precoding techniques have been proposed for 5G terrestrial networks and demonstrated effectiveness. However, their applications in NTN systems are limited. The main driven obstacle lies in the huge difference in the round-trip time (RTT) between terrestrial and satellite systems. As a result, the precoding method in the terrestrial system, which presumes instantaneous channel state information (CSI), cannot efficiently operate in outdated CSI in satellite networks. In addition, most of precoding methods for satellites are inherited from the terrestrial networks and assume the conventional payload architecture, which definitely does not fully exploit the potential of the flexible multi-beam payload.

Although the radio resource management has long been studied in satellite systems, see [3]–[5] and references therein, they mostly target beam-hopping and power allocation assuming the conventional payload with limited computation capability. With the advanced payload technology, digital transparent payload (DTP) [6] fully controls of spot beam coverage, frequency allocation and transmit power. Recently, there have been some works investigating the multiuser precoding techniques in non-geostationary orbit (NGSO) satellites based on the flexible payload capability. The authors of [7] proposed two schemes SatCP and SatHB for predicting effective downlink CSI and hybrid beamformers in massive multiple-input multiple-output (mMIMO) integrated low earth orbit (LEO) satellites using deep learning. In [8], a hybrid beamforming codebook is designed for mMIMO integrated LEO satellite operating in the Ku band, using a 2-D DFT-based grid of beams similar to 5G New Radio. The codebook aims to address coverage and availability issues in satellite-assisted terrestrial networks. The 5G-ALLSTAR project [9] proposed an interference management between satellite and terrestrial systems to leverage satellite-based terrestrial multi-connectivity (MC). The authors of [10] proposed solutions for spectrum sharing in a 5G cellular and satellite-terrestrial MC. These precoding designs fall into the non-codebook category, which requires knowledge of CSI at the transmitter, which can be a burden in NGSO due to the fast movement of satellites, especially LEO. To minimize the signaling overhead, the 3GPP standard suggests codebook-based design. A practical pre-computed precoders for massive multiuser MIMO systems was proposed in [11] called BeamRaster, which offers a fast and computation efficient solution. The authors of [12] investigated the codebook-based design in a spatial modulation system by proposing two codebooks, namely phase-only codebook and gain-only codebook. It was shown that both codebooks can effectively achieve the target performance with reduced complexity. Although not being proposed for satellite systems, this solution proves the scalability benefit of the codebook-based precoding.

The above-mentioned works either address the long RTT separately or considered the beamforming design under fixed bandwidth allocation setting. Our recent work showed that dynamic bandwidth allocation jointly with precoding design

improves the system sum rate, especially then the system is highly loaded [13]. In this work, we consider the flexible multibeam NGSO satellite which is capable of fully controlling the spot beam coverage, bandwidth and power allocation. Our contributions are as follows:

- We formulate the joint precoding design and bandwidth allocation problem to fully exploit the potentials of flexible multi-beam satellites under realistic long RTT to maximize the average system sum rate per service duration. The proposed design tackle the long RTT latency by jointly estimating the CSI using the Kalman filter and optimizing the precoding vectors and bandwidth allocated to each user group.
- We consider both the 3GPP-compatible codebook- and non-codebook-based methods. By adopting the Zero-forcing (ZF) based design, we convert the joint bandwidth and precoding design into a convex optimization problem with respect to the bandwidth and transmit power, which can be efficiently solved by standard methods.
- We evaluate the proposed design under practical system parameters using the system tool kit (STK) software [15]. Numerical results show that the proposed solution significantly improves the spot beam sum rate compared with the conventional channel estimation-based solution. In addition, the non-codebook precoding design achieves almost twice sum rate as the codebook-based precoding, at an expense of higher signaling overhead.

II. System Model and Problem Formulation

The considered system includes an NGSO (medium-earth orbit (MEO) or LEO) satellite serving ground terminal users (TUs) within its coverage, as depicted in Fig. II. By equipped with the advanced flexible payload technology, the NGSO satellite is capable of forming up to M spot beams with customized beam shapes with actual geographical distribution of TUs [6]. Because the spot beams are formed based on geographical locations of the TUs, and with advanced antenna technology, the inter-beam interference is negligible. Let K_m denote the number of TUs served by the m-th spot beam. Each spot beam is capable of providing a maximal N spatial multiplexing gain. Therefore, the channel gain between the satellite and generic single-antenna TU at spot beam m is modelled as $\boldsymbol{h}_k^m \in \mathcal{C}^{N\times 1}$. Unlike the spatial multiplexing technique in terrestrial network, e.g., massive MIMO, the spatial multiplexing gain in satellite system is generally small due to strong correlation among the satellite-user links. Typical value of N usually does not exceed 4, which is also suggested by the codebook-based precoding in 3GPP standard [1].

If the number of TUs K_m at spot beam m does not exceed N, they can be served simultaneously via multiuser precoding technique. Otherwise, the TUs will be divided into $G_m \triangleq \lceil K_m/N \rceil$ groups, and each user group does not have more than N TUs. Different groups will be served in orthogonal frequency bandwidth, whereas the TUs in the same group will be served in the same frequency bandwidth simultaneously via precoding technique.

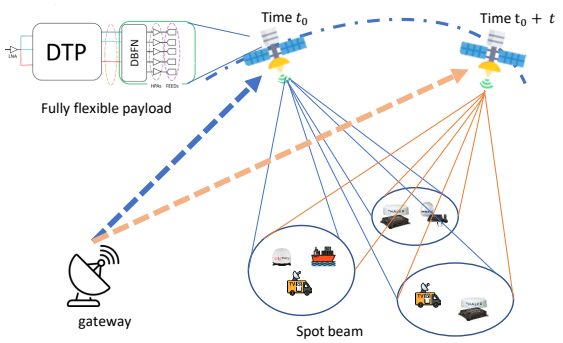

Fig. 1. The considered NGSO system with fully flexible multi-spot beam capability. Each service duration consists of T time slots.

A. Channel Model and Estimation

Due to the fast movement of the NGSO satellite, the channels between the satellite and TUs are time-varying. Each service duration of the satellite is divided into T time slots, in which the channel gain within one time slot is assumed to be quasi-static. Denote $\boldsymbol{h}_{k,g,m}^{(t)}$ as the channel gain from the satellite to the k-th TU belonging to group g of beam m at the t-th time slot. Denote $\mathbf{H}_m^{(t)} \triangleq [\boldsymbol{h}_{1,1,m}^{(t)}; \ldots; \boldsymbol{h}_{k,g,m}^{(t)}; \ldots; \boldsymbol{h}_{K_m,G_m,m}^{(t)}]^T \in \mathbb{C}^{K_m\times N}$ as the channel matrix from the satellite to all TUs in beam m, which can be expressed as [14]: $\mathbf{H}_m^{(t)} = \bar{\mathbf{H}}_m^{(t)} \circ \mathbf{F}_m^{(t)}$, where $\bar{\mathbf{H}}^{(t)} \in \mathbb{C}^{K_m\times N}$ represents the antenna radiation pattern and path loss, while the propagation effects are modeled by $\mathbf{F}^{(t)} \in \mathbb{C}^{K_m\times N}$ of which each entry is treated as a random variable.

1) Training Model: To estimate the channels, the system uses K τ-length orthogonal pilot sequences $\{\boldsymbol{\phi}_1, ..., \boldsymbol{\phi}_K\}$, with $\tau \geq K$. The training signal received at the gateway (GW) at time t, denoted by $\mathbf{Y}^{(t)} \in \mathbb{C}^{\tau\times N}$, can be expressed as

$$\mathbf{Y}^{(t)} = \sqrt{\rho\tau}\boldsymbol{\Psi}\mathbf{H}^{(t)} + \mathbf{Z}^{(t)}, \tag{1}$$

where $\boldsymbol{\Psi} \triangleq [\boldsymbol{\psi}_k]_{k\in\mathcal{K}} \in \mathbb{C}^{\tau\times K}$, satisfying the orthonormal condition as $\boldsymbol{\Psi}^H\boldsymbol{\Psi} = \tau\mathbf{I}_K$. The Gaussian noise is denoted as a matrix $\mathbf{Z}^{(t)}$ of which each entry is a random variable following $\mathcal{CN}(0,1)$.

2) Channel Estimation: To be simple, the training signal in (1) is rewritten as $\dot{\mathbf{y}}^{(t)} = \sqrt{\rho\tau}\ddot{\boldsymbol{\Psi}}\dot{\mathbf{h}}^{(t)} + \dot{\mathbf{z}}^{(t)}$, where a vector $\dot{\mathbf{x}}^{(t)}$ is the vectorization of the matrix $\mathbf{X}^{(t)}$, and $\ddot{\boldsymbol{\Psi}} \triangleq \mathbf{I}_N \otimes \boldsymbol{\Psi} \in \mathbb{C}^{\tau N\times KN}$. From the training signal $\dot{\mathbf{y}}^{(t)}$, the channel estimate can be computed using LMMSE, which is given as

$$\hat{\mathbf{h}}^{(t)} = \sqrt{\rho\tau}\ddot{\boldsymbol{\Psi}}^H\left(\mathbf{I}_{\tau N} + \rho\tau\ddot{\boldsymbol{\Psi}}\mathrm{diag}\left(\breve{\mathbf{h}}^{(t)}\right)\ddot{\boldsymbol{\Psi}}^H\right)^{-1}\dot{\mathbf{y}}^{(t)}, \tag{2}$$

where $\breve{\mathbf{h}}^{(t)}$ is vectorization of $\bar{\mathbf{H}}^{(t)}$, and $\mathrm{diag}(\mathbf{x})$ return a diagonal matrix with the main diagonal being vector $\mathbf{x}$.

B. Signal Transmission Model

To exploit the spatial multiplexing gain and the advanced flexible payload capability, a precoding vector $\boldsymbol{w}_{k,g,m}^{(t)}$ is applied to the data stream for TU k. Denote $s_{k,g,m}$ as the

data sent to user k at group g of beam m, then the received signal at user k in group g of beam m is given as:

$$y_{k,g,m}^{(t)} = (\boldsymbol{h}_{k,g,m}^{(t)})^H \boldsymbol{w}_{k,g,m}^{(t)} s_{k,g,m} + \sum\nolimits_{l \neq k} (\boldsymbol{h}_{k,g,m}^{(t)})^H \boldsymbol{w}_{l,g,m}^{(t)} s_{l,g,m} + n_{k,g,m}, \quad (3)$$

where the first element is the intended signal for user k, the second element is inter-user interference caused by other TUs in the same group g, and the last element is the Gaussian noise at the TU with noise density N_0. We note that since each user group g occupies an orthogonal bandwidth, there is no inter-group interference within one beam. Furthermore, since the beams are determined based on geographical locations of the TUs and with the advanced flexible multibeam payload, the inter-beam interference is assumed to be negligible.

Let $b_{g,m}$ denote the bandwidth allocated to the g-th group in beam m, the achievable rate of user k is given as follows:

$$r_{k,g,m}^{(t)} = b_{g,m} \log_2 \Big(1 + \frac{|(\boldsymbol{h}_{k,g,m}^{(t)})^H \boldsymbol{w}_{k,g,m}^{(t)}|^2}{\sum\limits_{l \neq k} |(\boldsymbol{h}_{k,g,m}^{(t)})^H \boldsymbol{w}_{l,g,m}^{(t)}|^2 + b_{g,m} N_0}\Big).$$

C. Problem formulation

We would like to jointly optimize the precoding vector design and bandwidth allocation to maximize the system sum rate, subject to individual TU's QoS requirement:

$$\underset{\{\boldsymbol{w}_{k,g,m}^{(t)}, b_{g,m}\}}{\texttt{maximize}} \quad \frac{1}{T} \sum\nolimits_{t=1}^{T} \sum\nolimits_{k,g,m} r_{k,g,m}^{(t)} \quad (4)$$

$$\texttt{s.t.} \quad r_{k,g,m}^{(t)} \geq \eta_{k,g,m}, \forall k, g, m, t; \ \sum\nolimits_{g} b_{g,m} \leq B, \forall m \quad (4a)$$

$$\sum\nolimits_{k,g} \|\boldsymbol{w}_{k,g,m}^{(t)}\|^2 \leq P_{\Sigma,m}, \forall m, t, \quad (4b)$$

where B is the total frequency bandwidth and $P_{\Sigma,m}$ is the total transmit power at beam m. In (4), the first constraint is to satisfy the TU's minimum QoS requirement $\eta_{k,g,m}$ and total bandwidth constraint; constraint (4b) limits the total transmit power at each beam cannot exceed the maximum power.

Challenges in solving (4): The difficulty of solving problem (4) lies in not only the non-concavity of the achievable rate function (with respect to both precoding vector $\boldsymbol{w}_{k,g,m}^{(t)}$ and the bandwidth $b_{g,m}$) but also the lack of channel state information for designing the precoding vectors. In fact, in order to design $\boldsymbol{w}_{k,g,m}^{(t)}$, it requires to know the CSI at time slot t. Unlike in terrestrial networks in which the propagation delay is negligible, the RTT in satellite systems cannot be ignored. This long RTT causes a delayed CSI issue in which the precoding vectors designed at time slot t is based on the CSI estimated at previous time slot.

III. Proposed Joint Channel Estimation, Precoding and Bandwidth Allocation

A straightforward way to solve (4) is to employ the channel estimated at time slot t to design the precoding vectors for data transmission at time slot $t+1$, i.e., $\boldsymbol{w}_{k,g,m}^{(t+1)}(\hat{\mathbf{h}}_{k,g,m}^{(t)})$. In the fast-fading environment and long RTT, however, the real channels in data transmission clearly distinguish from the channel estimated previously. This method could results in a very sup-optimal solution, as we will show in later sections. To overcome this challenge, this section will present the channel prediction and precoding design to adapt with the change in environment condition.

A. Kalman Filter-based Channel Predictor

In the Kalman filter, the sequential channels are successively predicted, using p-order auto-regression model. Accordingly, the sequence of predicted channels at time t can be expressed as $\hat{\mathbf{g}}^{(t+1)} = \boldsymbol{\Xi}^{(t)} \hat{\mathbf{g}}^{(t)} + \boldsymbol{\Theta}^{(t)} \mathbf{u}^{(t)}$, where the concatenated sequence of p channel vectors at p consecutive time slots, $\hat{\mathbf{g}}^{(t)} \triangleq \big[(\hat{\mathbf{h}}^{(t)})^H \ \cdots \ (\hat{\mathbf{h}}^{(t-p+1)})^H\big]^H \in \mathbb{C}^{KNp \times 1}$. The parameter matrix $\boldsymbol{\Theta}^{(t)}$ is generalized as $\boldsymbol{\Theta}^{(t)} \triangleq \big[\sqrt{1-\xi}\mathbf{I}_{KN}, \ \mathbf{0}_{KN \times KN}, \ \ldots, \ \mathbf{0}_{KN \times KN}\big]^T \in \mathbb{C}^{KNp \times KN}$ and $\boldsymbol{\Xi}^{(t)} \triangleq \Big[\sqrt{\xi}\bar{\boldsymbol{\Xi}} \ \ \sqrt{\xi}\tilde{\boldsymbol{\Xi}}; \ \mathbf{I}_{KN(p-1)} \ \ \mathbf{0}_{KN(p-1) \times KN}\Big]$, where ξ represents the correlation coefficient. The matrices $\bar{\boldsymbol{\Xi}} \in \mathbb{C}^{KN(p-1) \times KN}$ and $\tilde{\boldsymbol{\Xi}} \in \mathbb{C}^{KN \times KN}$ are determined as $\big[\bar{\boldsymbol{\Xi}} \ \ \tilde{\boldsymbol{\Xi}}\big] \triangleq \big[\mathbf{C}_1 \ \cdots \ \mathbf{C}_p\big]\bar{\mathbf{C}}^{-1}$, where the covariance matrices, $\mathbf{C}_i, \ i = 0, 1, \cdots, p$, and $\bar{\mathbf{C}}$ are given as $\mathbf{C}_i = \mathbb{E}\big[\mathbf{g}^{(t)}(\mathbf{g}^{(t-i)})^H\big]$ and

$$\bar{\mathbf{C}} = \begin{bmatrix} \mathbf{C}_0 & \mathbf{C}_1 & \cdots & \mathbf{C}_{p-1} \\ \mathbf{C}_1 & \mathbf{C}_0 & \cdots & \mathbf{C}_{p-2} \\ \vdots & \vdots & \ddots & \vdots \\ \mathbf{C}_{p-1} & \mathbf{C}_{p-2} & \cdots & \mathbf{C}_0 \end{bmatrix}.$$

B. Joint Precoding Design and Bandwidth Allocation

After channel estimation, we can obtain the estimate channel gain at time slot $t+1$, which will be used to design the precoding vectors. Therefore, the original problem (4) can be decoupled in to sub-problem for every time slot. In addition, because the radio resource management is analogy in all spot beams, we drop the time slot and beam indexes for ease of presentation. Thus, the joint precoding design and bandwidth allocation for a particular time slot and spot beam becomes:

$$\underset{\{\boldsymbol{w}_{k,g}, b_g\}}{\texttt{maximize}} \quad \sum\nolimits_{k,g} r_{k,g} \quad (5)$$

$$\texttt{s.t.} \quad \sum\nolimits_{k,g} \|\boldsymbol{w}_{k,g}\|^2 \leq P_\Sigma r_{k,g} \geq \eta_{k,g}, \forall k, g; \ \sum\nolimits_{g} b_g \leq B,$$

where $r_{k,g} = b_g \log_2(1 + \frac{|\boldsymbol{h}_{k,g}^H \boldsymbol{w}_{k,g}|^2}{\sum_{l \neq k} |\boldsymbol{h}_{k,g}^H \boldsymbol{w}_{l,g}|^2 + b_g N_0})$ and note that $\boldsymbol{w}_{k,g}$ is designed based on the predicted channels $\hat{\boldsymbol{h}}$.

We consider both codebook- and non-codebook based precoding designs suggested by the 3GPP New Radio standardization [2].

1) Non-codebook based precoding design: The non-codebook based design is implemented in TM8 and TM9, which require high-resolution feedback of the CSI. We consider a zero-forcing based precoding design due to its low computation complexity. Under the ZF-based design, the precoding vector for user k in the group g is given as $\boldsymbol{w}_g^{ZF} = \sqrt{p_{k,g}}\tilde{\boldsymbol{w}}_{k,g}$, where $p_{k,g}$ is the power factor and $\tilde{\boldsymbol{w}}_{k,g}$ the g-th column of the ZF precoding matrix $\mathbf{W} = \hat{\mathbf{H}}^{(t+1)}\Big(\big(\hat{\mathbf{H}}^{(t+1)}\big)^H \hat{\mathbf{H}}^{(t+1)}\Big)^{-1}$. It is noted that under the ZF-based design, the inter-user interference within each group is mitigated, i.e., $|\boldsymbol{h}_{l,g}^H \boldsymbol{w}_{k,g}^{ZF}| = \delta_{k,l} p_{k,g}$. Since the phase of the

precoding vectors is predefined, the joint problem (5) becomes the joint bandwidth and power allocation, which is stated as follows:

$$\begin{aligned} \underset{\{p_{k,g},b_g\}}{\texttt{maximize}} \quad & \sum\nolimits_{k,g} b_g \log_2(1+\frac{p_{k,g}}{b_g N_0}) \\ \texttt{s.t.} \quad & \text{constraints of problem (5).} \end{aligned} \tag{6}$$

Proposition 1: For an arbitrary positive constant a, the function $f(x,y) = x\log(1+ay/x)$ is jointly concave in $\mathcal{R}^+ \times \mathcal{R}^+$.

The proof of Proposition 1 can be obtained by taking the second-order derivative of $f(x,y)$. Since the objective function in (6) is concave and all constraints are either linear or convex, the optimization problem (6) is convex, and thus can be efficiently solved using standard methods, e.g., interior point.

2) Codebook-based precoding design: While the non-codebook based design promises higher spectral efficiency, it requires high-resolution feedback of the CSI. The codebook-based design, on the other hand, minimizes the signaling overhead via predefined precoding matrices. Currently, the multiuser precoding is enabled in TM5 (supports 2 users) and TM8 (supports up to 4 users). For example, in a 4 transmit antennas case, the codebook includes 16 precoding matrices, in which the n-th precoding matrix is computed as $\mathbf{W}_n = \mathbf{I} - 2\frac{\mathbf{u}_n^H \mathbf{u}_n}{\mathbf{u}_n \mathbf{u}_n^H}$, where $\mathbf{u}_n$ is the n-th vector resulting from all combinations of $[\pm 1, \pm j, \pm\frac{1+j}{\sqrt{2}}, \pm\frac{1-j}{\sqrt{2}}]$. To minimize the signaling overhead, the frequency bandwidth is equally allocated to the user groups. Therefore, the achievable rate of user k in group g, given the precoding vector $\boldsymbol{w}_{\mathrm{CB},k,g}$, is $r_{k,g}(\boldsymbol{w}_{\mathrm{CB},k,g}) = \frac{B}{G} \times \log_2\left(1 + \frac{P_\Sigma |\boldsymbol{h}_{k,g}^H \boldsymbol{w}_{\mathrm{CB},k,g}|^2}{\sum_{l\neq k} |\boldsymbol{h}_{k,g}^H \boldsymbol{w}_{\mathrm{CB},l,g}|^2 + \frac{BKN_0}{G}}\right)$. It is noted that the 3GPP determines the precoding vectors as the first K columns of the predefined precoding matrix. In order to improve the system performance, we can heuristically search over all $\binom{N}{K}$ combinations. The steps of codebook-based precoding design are given in Algorithm 1.

Algorithm 1 Codebook-based precoding design

Inputs: number of users K, CSI estimation/feedback
Outputs: the precoding vector indexes
1. For each precoding codebook matrix $\mathbf{W}$, there $K!\binom{N}{K}$ mappings K users to the K columns of $\mathbf{W}$
2. For each mapping, compute sum rate $r_{k,g}(\boldsymbol{w}_{\mathrm{CB},k,g})$
3. Select the precoding matrix and corresponding mapping that maximizing the sum rate
4. Inform the users the precoding matrix indicator (PMI) and mapping

IV. Performance Evaluation on Realistic System Parameters

In this section, we conduct simulations results to demonstrate the performance of the proposed design. We consider the Iridium LEO satellite [16] that operates at an orbit of 780 km with each service duration is 10 minutes. With the time slot duration of 2 seconds, each service duration has $T = 300$ time slots. The LEO covers an area with a radius of 500 km and each spot beam has a minimum radius of 50 km. The bandwidth $B = 20$MHz and $N = 4$. The number of users per spot beam $K_m = 3 \to 6, \forall m$, and the pilot sequence length $\tau = K_m$. Other parameters are selected in such a way that the free space pathloss is matched with the values provided by the STK software , in which the pathloss is between 173dB and 185dB [15]. The small-scale fading $\mathbf{F}_m^{(t)}$ is modelled by the first-order Markov chain $\mathbf{F}_m^{(t)} = \sqrt{\xi}\mathbf{F}_m^{(t-1)} + \sqrt{1-\xi}\mathbf{Z}$, where ξ is the correlation coefficient and $\mathbf{Z} \sim \mathcal{CN}(0, \mathbf{I})$.

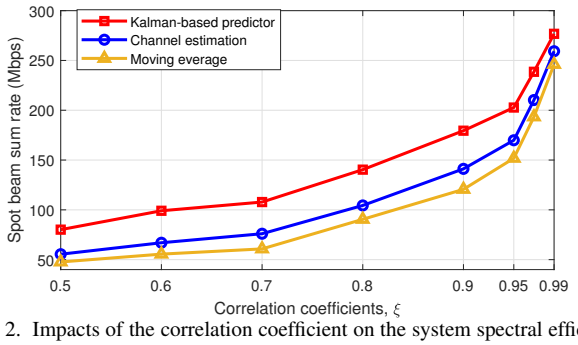

Fig. 2. Impacts of the correlation coefficient on the system spectral efficiency. The satellite transmit power is 20 dBW.

A. Impact of the channel correlation coefficient

Fig. 2 plots the average sum rate per spot beam as a function of the correlation coefficient. Intuitively, smaller the correlation coefficient is, the slower the channel coefficient varies over time. To demonstrate the effectiveness of the proposed channel prediction based on Kalman filter, two other curves are also presented. The first curve is the conventional channel estimation scheme without prediction, which is named *Channel estimation* in the figure. The second scheme is *Moving average*, which utilizes the average of the last t_{hist} channels to compute the precoding vectors. All schemes employ the design in Sec. III-B1 to get the precoding vectors. The benefit of the proposed prediction is clearly shown via superior sum rate performance compared to two reference schemes. In general, the channel prediction boosts the average sum rate by 40 Mbps. When the correlation coefficient increases, all the schemes achieve a higher sum rate. This is because in the channel is strongly correlated, then both the channel prediction and estimation are more efficient.

B. Non-codebook and codebook precoding performance

We compare the performance of the non-codebook and codebook-based designs described in Sec. III. In order to show the channel prediction advantage, the non-codebook precoding design is also applied to the estimated channel without prediction, which is named *Non-codebook: Channel estimation* in the figure.

Fig. 3 presents the average spotbeam sum rate for different transmit power values. having larger transmit powers in general boosts the system sum rate. At small transmit power values, all schemes perform closely. As the transmit power increases, the relative gain between the non-codebook and codebook-based designs is also enlarged. This is because in the codebook-based design, the precoding vectors are selected from the given codebook. This implies that the inter-user interference cannot be completely mitigated. In such case,

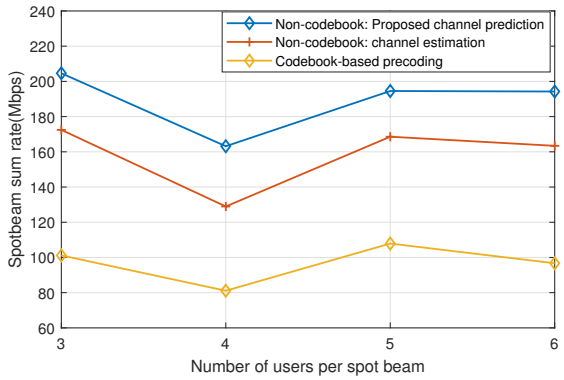

Fig. 4. Average spot-beam sum rate as a function of the number of users. The transmit power is 20 dB.

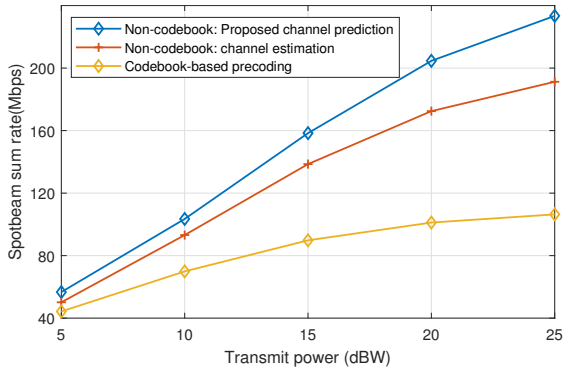

Fig. 3. Average spot-beam sum rate as a function of the transmit power. Each spot beam is serving 3 UEs.

increasing the transmit power also increases the inter-user interference. At a transmit power of 20 dBW, the proposed non-codebook design achieves twice the sum rate as the codebook-based scheme. In addition, the proposed channel prediction improves the sum rate by 25% compared with the scheme using only the channel estimation. It is worth to note that the codebook-based precoding design offers the minimum signaling overhead since only the precoding matrix indicator is exchanged.

Fig. 4 shows the sum rate as a function of the number of users per spot beam. The total transmit power is fixed at 20 dBW. It is clearly shown in the figure the advantage of the non-codebook precoding design compared with the codebook-based scheme. We observe that the sum rate degrades at $K = 4$ users in all schemes and then increases with the number of users. This is because when $K = 4$, all users are simultaneously served, resulting in higher inter-user interference in the codebook-based design and less efficiency of inter-user interference cancellation in the non-codebook precoding design. When $K > 4$, the total users is divided into two user groups, each having less than 4 users. Thus the inter-user inference mitigation is more efficient in these cases. We note that the total transmit power is fixed, therefore the sum rate does not increase as K increases.

V. Conclusion and Discussion

In this paper, we have studied the 3GPP precoding designs in NGSO satellite systems which take into considerations of the long round-trip time latency. By equipped with the advanced flexible payload technology, the NGSO satellite is capable of performing base-band signal processing and radio resource allocation. To tackle the long RTT, we proposed a joint channel prediction and precoding vector design to maximize the average system sum rate. We considered both codebook-based precoding design, which offers the minimum signaling overhead, and the non-codebook Zero-forcing based precoding design. We used the system tool kit (STK) software to obtain realistic channel pathloss for numerical simulation. We demonstrated that the non-codebook design can achieves twice the sum rate as the codebook-based solution at the expense of higher signaling overhead and that the proposed prediction solution achieve up to 25% higher sum rate compared with the conventional channel estimation method.

Acknowledgment

This work is supported by the Luxembourg National Research Fund via project FNR RUTINE, ref. FNR/C22/IS/17220888/RUTINE, and project FNR INSTRUCT, ref. FNR/IPBG19/14016225/INSTRUCT.

References

[1] Rel-17 RP-201256: Solutions for NR to support non-terrestrial networks.
[2] RP-181370, "Study on solutions evaluation for NR to support Non Terrestrial Network," 3GPP RAN80, June 2018.
[3] M. Á. Vázquez et al., "Precoding in Multibeam Satellite Communications: Present and Future Challenges," in *IEEE Wireless Communications*, vol. 23, no. 6, pp. 88-95, Dec. 2016.
[4] P. Angeletti and R. De Gaudenzi, "A Pragmatic Approach to Massive MIMO for Broadband Communication Satellites," in *IEEE Access*, vol. 8, pp. 132212-132236, 2020.
[5] O. Kodheli et al., "Satellite Communications in the New Space Era: A Survey and Future Challenges," *IEEE Communications Surveys& Tutorials*, vol. 23, no. 1, pp. 70-109, Q1. 2021.
[6] Glyn Thomas, "Enabling Technologies for flexible HTS payloads," in *Proc. 33th AIAA Int. Commun. Satellite Systems Conf.*, AIAA 2015-4348.
[7] Y. Zhang, A. Liu, P. Li, and S. Jiang, "Deep Learning (DL)-Based Channel Prediction and Hybrid Beamforming for LEO Satellite Massive MIMO System," in *IEEE Internet of Things Journal*, vol. 9, no. 23, pp. 23705-23715, Dec. 2022.
[8] J. Palacios, N. Gonzalez-Prelcic, C. Mosquera, T. Shimizu, and C.-H. Wang, "A hybrid beamforming design for massive MIMO LEO satellite communications," in *Front. Space Technol.*, 2:696464, 2021.
[9] N. Cassiau et al., "5G-ALLSTAR: Beyond 5G Satellite-Terrestrial Multi-Connectivity," in *Proc. Joint European Conference on Networks and Communications*, 2022, pp. 148–153.
[10] N. Cassiau et al., "Satellite and Terrestrial Multi-Connectivity for 5G: Making Spectrum Sharing Possible," in *Proc. IEEE Wireless Commun. Netw. Conf.*, 2020, pp. 1-6.
[11] M. Meng et al., "BeamRaster: A Practical Fast Massive MU-MIMO System With Pre-Computed Precoders," in *IEEE Transactions on Mobile Computing*, vol. 18, no. 5, pp. 1014-1027, May 2019.
[12] E. Sourour, "Codebook-based precoding for generalized spatial modulation with diversity," in *EURASIP J Wireless Com Network*, 2019, 229 (2019).
[13] T. X. Vu, S. Chatzinotas, and B. Ottersten, "Dynamic Bandwidth Allocation and Precoding Design for Highly-Loaded Multiuser MISO in Beyond 5G Networks," in *IEEE Transactions on Wireless Communications*, vol. 21, no. 3, pp. 1794 – 1805, Mar. 2022.
[14] A. I. Perez-Neira, M. A. Vazquez, M. R. B. Shankar, S. Maleki and S. Chatzinotas, "Signal Processing for High-Throughput Satellites: Challenges in New Interference-Limited Scenarios," in *IEEE Signal Processing Magazine*, vol. 36, no. 4, pp. 112-131, July 2019.
[15] STK software, https://www.agi.com/products/stk
[16] Iridium Networks, Online: https://www.iridium.com/network/